Study of rare $B_c^+ \to D_{d,s}^{(*)+} l\bar{l}$ decays

C. Q. Geng

Department of Physics, National Tsing Hua University, Hsinchu, Taiwan, Republic of China
and Theory Group, TRIUMF, 4004 Wesbrook Mall, Vancouver, B.C., Canada V6T 2A3

C. W. Hwang

Department of Physics, National Tsing Hua University, Hsinchu, Taiwan, Republic of China

C. C. Liu

Department of Physics, National Tsing Hua University, Hsinchu, Taiwan, Republic of China
and Theory Group, TRIUMF, 4004 Wesbrook Mall, Vancouver, B.C., Canada V6T 2A3

We study the rare decays of $B_c^+ \to D_q^{(*)+} l\bar{l}$ ($q=d,s$ and $l=\nu_l, e, \mu, \tau$) in the standard model. The form factors are evaluated in the light front and constituent quark models, respectively. We find that the decay branching ratios calculated in the two models for $B_c^+ \to D_q^+ l\bar{l}$ agree well with each other, whereas those for $B_c^+ \to D_q^{*+} l\bar{l}$ are different.

I. INTRODUCTION

Recently, the Collider Detector at Fermilab (CDF) Collaboration has observed the bottom-charm B_c meson at the Tevatron in Fermilab [1,2]. Its mass and lifetime are given as $M_{B_c} = 6.40 \pm 0.39$ GeV and $\tau_{B_c} = (0.46^{+0.18}_{-0.16}) \times 10^{-12}$s, respectively. The study of the B_c meson is quite interesting due to the following four main reasons: (i) B_c is the lowest bound state of two heavy quarks (b and c) with open (explicit) flavor. It can be compared with the hidden (implicit) flavor ($\bar{c}c$) charmonium and ($\bar{b}b$) bottomonium. The hidden-flavor states decay strongly and electromagnetically whereas the B_c meson does so weakly because it is below the $B\bar{D}$ threshold. (ii) One may expect that the weak decays of the B_c meson are similar to those of $B_{u,d,s}$ mesons. However, the major difference between the weak decay properties of B_c and $B_{u,d,s}$ is that those of the latter ones are described very well in the framework of the heavy quark limit. In this limit the weak decay form factors are blind to the flavor and spin orientation of the heavy quark. All of them can be expressed through a single Isgur-Wise function [3]. In the case of B_c, the heavy flavor and spin symmetries must be reconsidered because both b and c quarks are heavy. Thus the study with the finite quark mass is a more appropriate way. (iii) There have been many investigations of rare radiative, leptonic and semileptonic decays of $B_{u,d,s}$ mesons induced by the flavor-changing neutral current transitions of $b \to s, d$ [4] since the CLEO observation [5] of $b \to s\gamma$. More recently, the process of $B \to K\mu^+\mu^-$ has been also seen [6] at the Belle detector in the KEKB e^+e^- storage ring. In the standard model (SM), these transitions are forbidden at the tree level and occur only through loop diagrams. The studies are even more complete if similar decays for B_c are also included, which can be achieved by introducing the spectator quark of c in the diagrams. In fact, some of the works have been done and they can be found in Refs. [7–10]. (iv) It is believed that there are

about $10^8 - 10^9 B_c$ mesons to be produced in future experiments at hadronic colliders [11], such as the BTeV and CERN LHC-B experiments [12]. In these experiments, most rare B_c decays should be accessible.

In this paper, we will concentrate on the rare decays of $B_c^+ \to D_q^{(*)} l\bar{l}$ ($q=d,s$) due to the $b \to q$ transitions as shown in Fig. 1 in the SM, which have not yet been explored in the literature. To study their decay rates and branching ratios, we need to calculate the transition form factors of the vector, axial-vector, and tensor currents, which must be treated with the nonperturbative method. There are many different candidates for this purpose, e.g., lattice QCD [13], QCD sum rule
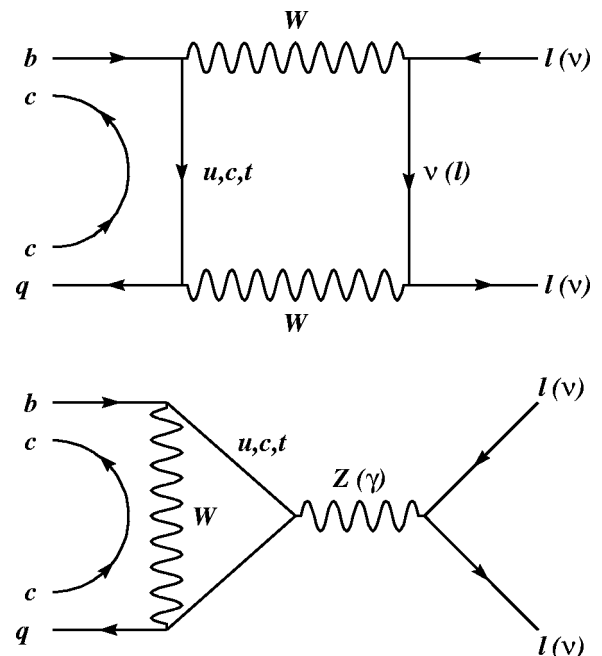

FIG. 1. One-loop diagrams for the short-distance contributions to the decays of $B_c^+ \to D_q^{(*)+} l\bar{l}(q=d,s)$ in the SM.

[14,15], and phenomenological models. In this work, we use the frameworks of two phenomenological models: the light front quark model (LFQM) [16,17] and the constituent quark model (CQM) [18,19], to evaluate the form factors.

This paper is organized as follows. In Sec. II, we calculate the form factors for $B_c^+ \rightarrow D_{d,s}^{(*)+}$ transitions in the LFQM and CQM. In Sec. III, we study the differential rates and branching ratios of $B_c^+ \rightarrow Pl\bar{l}$ and $B_c^+ \rightarrow Vl\bar{l}$ decays with $l = \nu, e, \mu, \tau$ and $P(V) =$ pseudoscalar (vector) meson, respectively. We also compare the results in the two models. Our conclusions are given in Sec. V.

II. FORMALISM AND MODELS

A. Matrix elements

To get the transition matrix elements of $B_c^+ \rightarrow P(V)$ with various quark models, we parametrize them in terms of the relevant form factors as follows:

$$\langle P(p_2)|V_\mu|B_c(p_1)\rangle = F_+(q^2)P_\mu + F_-(q^2)q_\mu,$$

$$\langle P(p_2)|T_{\mu\nu}q^\nu|B_c(p_1)\rangle = \frac{1}{m_{B_c} + m_P}$$
$$\times [q^2 P_\mu - (P \cdot q)q_\mu]F_T(q^2),$$

$$\langle V(p_2,\epsilon)|V_\mu \mp A_\mu|B_c(p_1)\rangle$$
$$= \frac{1}{m_{B_c} + m_V}[-iV(q^2)\varepsilon_{\mu\nu\alpha\beta}\epsilon^{*\nu}P^\alpha q^\beta$$
$$\pm A_0(q^2)(P \cdot q)\epsilon_\mu^* \pm A_+(q^2)(\epsilon^* \cdot P)P_\mu$$
$$\pm A_-(q^2)(\epsilon^* \cdot P)q_\mu],$$

$$\langle V(p_2,\epsilon)|(T_{\mu\nu} \pm T_{\mu\nu}^5)q^\nu|B_c(p_1)\rangle$$
$$= -ig(q^2)\varepsilon_{\mu\nu\alpha\beta}\epsilon^{*\nu}P^\alpha q^\beta \pm a_0(q^2)(P \cdot q)$$
$$\times \left[\epsilon_\mu^* - \frac{1}{q^2}(\epsilon^* \cdot q)q_\mu\right] \pm a_+(q^2)(\epsilon^* \cdot P)$$
$$\times \left[P_\mu - \frac{1}{q^2}(P \cdot q)q_\mu\right], \qquad (1)$$

where m_i ($i = B_c, P, V$) are the meson masses, $p_1(p_2)$ is the momentum of the initial (final) meson, ϵ is the vector meson polarization vector, $P = p_1 + p_2$, $q = p_1 - p_2$, $V_\mu = \bar{q}_2\gamma_\mu q_1$, $A_\mu = \bar{q}_2\gamma_\mu\gamma_5 q_1$, $T_{\mu\nu} = \bar{q}_2 i\sigma_{\mu\nu}q_1$, $T_{\mu\nu}^5 = \bar{q}_2 i\sigma_{\mu\nu}\gamma_5 q_1$, and $F_{\pm,T}$, V, $A_{0,\pm}$, g, and $a_{0,\pm}$ are the form factors.

Since the calculations of the transition form factors in Eq. (1) belong to the nonperturbative regime, the phenomenological quark models may be needed. One thing worth mentioning here is that all of the form factors will be studied in the timelike physical meson decay region of $0 \leq q^2 \leq (m_{B_c} - m_{P(V)})^2$. As q^2 decreases (corresponding to the increasing recoil momentum), we have to start considering relativistic effects seriously. In particular, at the maximum recoil point

of $q^2 = 0$ where the final meson could be highly relativistic, there is no reason to expect that the nonrelativistic quark model is still applicable. A consistent treatment of the relativistic effects of the quark motion and spin in a bound state is a main issue of the relativistic quark model.

B. LFQM

The LFQM [20,21] is the relativistic quark model in which a consistent and fully relativistic treatment of quark spins and the center-of-mass motion can be carried out. This model has many advantages. For example, the light-front wave function is manifestly Lorentz invariant as it is expressed in terms of the momentum fraction variables (in "+" components) in analog to the parton distributions in the infinite momentum frame. Moreover, hadron spin can also be correctly constructed by using the so-called Melosh rotation. The kinematic subgroup of the light-front formalism has the maximum number of interaction-free generators including the boost operator which describes the center-of-mass motion of the bound state (for a review of the light-front dynamics and light-front QCD, see Ref. [22]).

The LFQM has been applied to study the heavy-to-heavy and heavy-to-light weak decay form factors in the timelike region [16,23]. These calculations are based on the observation [24] that in the frame where the momentum transfer is purely longitudinal, i.e., $q_\perp = 0$, $q^2 = q^+ q^-$ covers the entire range of momentum transfers. The price one has to pay is that, besides the conventional valence-quark contribution, one must also consider the nonvalence configuration (or the so-called Z graph) arising from the quark-pair creation in the vacuum. Unfortunately, a reliable way of estimating the Z graph is still lacking. However, the nonvalence contribution vanishes if $q^+ = 0$, and it is supposed to be unimportant for heavy-to-heavy transitions [16]. In this paper, all of the values obtained from the LFQM are based on the formulas in Refs. [16,17]. We note that the form factors in Eq. (1) depend on the meson ($H = q_1\bar{q}_2$) wave functions Φ_H. To fix the parameters in the wave functions, one may use the meson decay constants f_H, given by

$$f_H = \sqrt{24} \int \frac{dx \, d^2k_\perp}{2(2\pi)^3} \Phi_H(x, k_\perp) \frac{\mathcal{A}}{\sqrt{\mathcal{A}^2 + k_\perp^2}}, \qquad (2)$$

where $\mathcal{A} = m_{q_1}x + m_{q_2}(1-x)$ with m_{q_i} being the quark masses and $\vec{k}_\perp$ is the component of the internal momentum $\vec{k} = (\vec{k}_\perp, k_z)$.

C. CQM

As mentioned in Sec. I, there are also other theoretical approaches for calculating the form factors. However, the theoretical uncertainties are large and each of these methods has only a limited range of applicability. For example, the model with QCD sum rules gives good results for the form factors at the low q^2 region; whereas the lattice QCD is appropriate only at the high q^2 one. In spite of the fact that
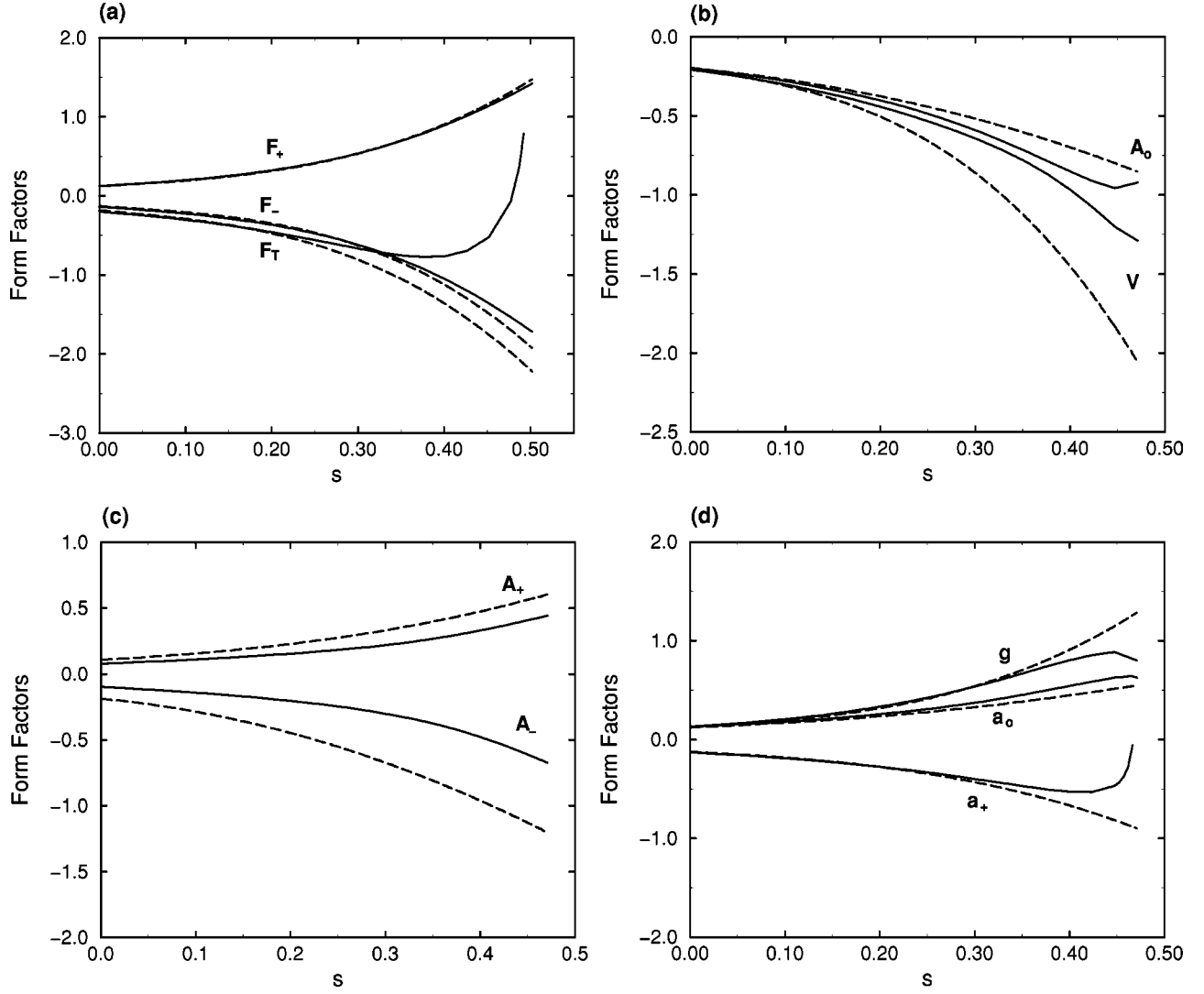
FIG. 2. Form factors of (a) $F_{\pm,T}$ for $B_c^+ \to D^+$, and (b) V and A_0, (c) $A_\pm$, and (d) g and $a_{0,+}$ for $B_c^+ \to D^{*+}$. The solid and dashed curves stand for the results from the LFQM and CQM, respectively.

the quark models can be used to evaluate the form factors in the full q^2 range, they are not closely related to the QCD Lagrangian and have many input parameters which are not measurable directly. Therefore, a relativistic constituent quark model is suggested in Ref. [25] which combines several theoretical methods such as the constituent quark models, QCD sum rules, lattice QCD calculations, and analytical constraints. This model used the light-cone technique with the relativistic double spectral representations in the initial and final meson wave functions. Explicitly, they calculated the form factors at $q^2 < 0$, i.e. the spacelike region, by choosing $P_\perp = 0$, $q_+ = 0$, and $q_\perp^2 = -q^2$. In order to obtain the form factors in the $q^2 > 0$ region, in Ref. [25], some modifications from the spacelike formulas were used to get their values in $0 < q^2 < (m_b - m_{d,s})^2$. It is known that in the timelike region $q^2 > 0$, there are the normal and anomalous parts, respectively. The result for the former is the same as that for $q^2 < 0$, but for the latter it can be ignored for small $q^2 > 0$ and rises sharply as $q^2 \to (m_b - m_{d,s})^2$.

In this paper, we will evaluate the form factors of $B_c^+ \to D_{d,s}^{(*)+}$ in the CQM by using the results in Refs. [18,19]. In the calculations, we first compute the values for the normal parts in $0 < q^2 < (m_b - m_{d,s})^2$ and then fit the data in terms of the double pole form, given by

$$F_i(q^2) = \frac{F_i(0)}{1 + \sigma_1 s + \sigma_2 s^2} \qquad (3)$$

where $s = q^2/m_{B_c}^2$, $F_i(0)$ are the form factors at $q^2 = 0$, and $\sigma_{1,2}$ are the fitted parameters. The form factors in the remaining regions of $(m_b - m_{d,s})^2 \leqslant q^2 \leqslant (m_{B_c} - m_{P,V})^2$ can be extrapolated from Eq. (3).

D. Form factors

As in Refs. [16–19], in this paper we choose the Gaussian-type meson wave function for both LFQM and CQM to calculate the form factors, i.e.,
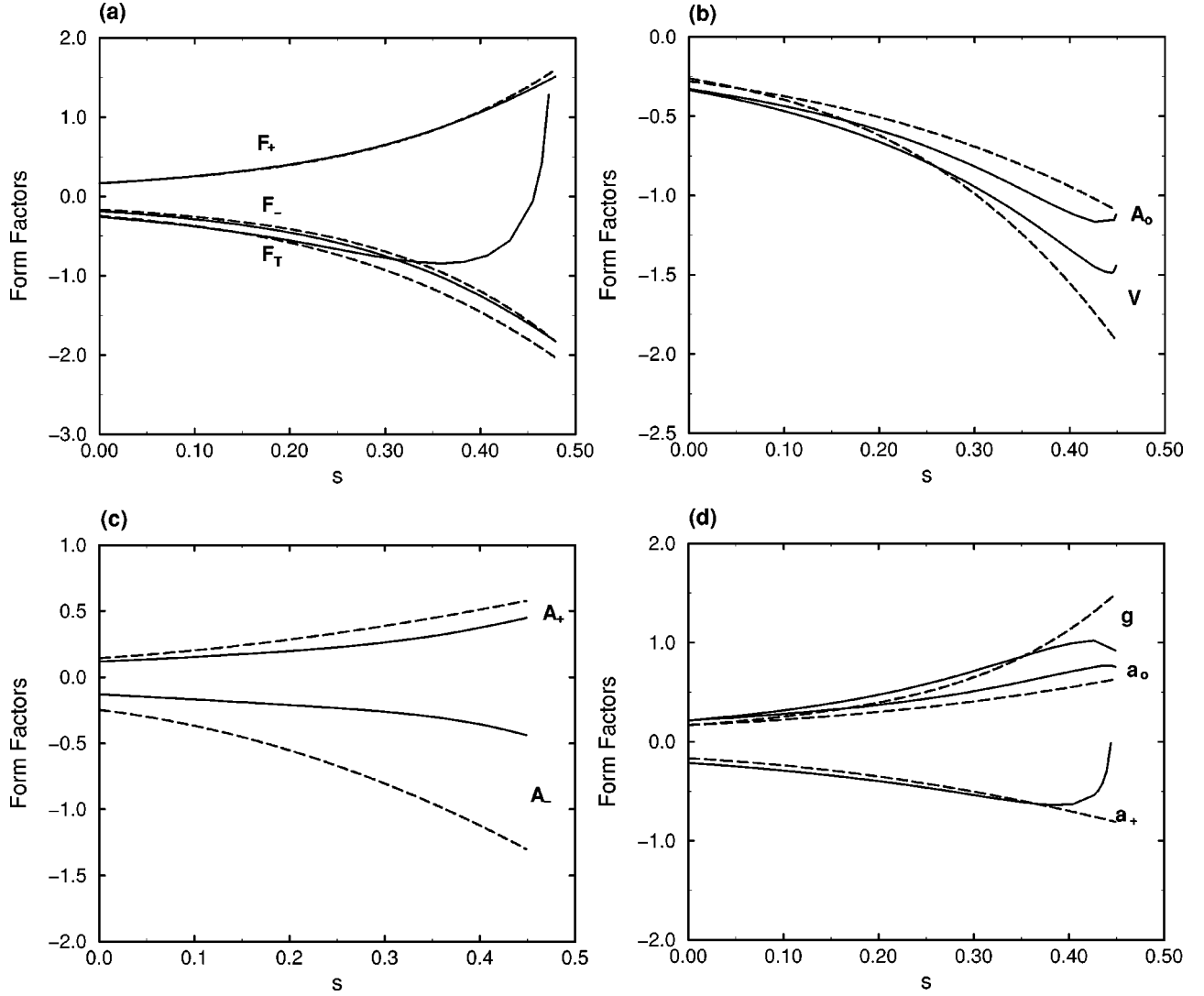
FIG. 3. Same as Fig. 2 but replacing $D^{(*)}$ by $D_s^{(*)}$.

$$\Phi_H \propto \exp\left(-\frac{\vec{k}^2}{2\omega_H^2}\right), \qquad (4)$$

where $\vec{k}$ and ω_H are the internal momentum and the scale parameter of H meson, respectively.

To find the numerical values of the form factors in the two models, we need to specify the parameters appearing in the wave functions. In the LFQM, we use the decay constants to constrain the quark masses and ω_H in Eq. (4) [16]. However, since the decay constants of heavy mesons are unknown experimentally, we have to rely on results in other QCD models such as the lattice QCD. Explicitly, we take [2,8]

$$f_{B_c} = 360 \text{ MeV}, \quad f_{D_d} = 200 \text{ MeV}, \quad f_{D_d^*} = 250 \text{ MeV},$$

$$f_{D_s} = 230 \text{ MeV}, \quad f_{D_s^*} = 330 \text{ MeV}, \quad m_d = 0.25 \text{ GeV},$$

$$m_s = 0.40 \text{ GeV}, \quad m_c = 1.60 \text{ GeV}, \quad m_b = 4.80 \text{ GeV}, \qquad (5)$$

which fix the scale parameters to be

$$\omega_{B_c} = 0.81 \text{ GeV}, \quad \omega_{D_d} = 0.46 \text{ GeV}, \quad \omega_{D_d^*} = 0.47 \text{ GeV},$$

$$\omega_{D_s} = 0.50 \text{ GeV}, \quad \omega_{D_s^*} = 0.56 \text{ GeV}, \qquad (6)$$

respectively. In our calculations, we also take $m_{B_c} = 6.4$ GeV and $\tau_{B_c} = 0.46 \times 10^{-12}$ s. In order to compare the numerical values in the LFQM and CQM, we shall use the same decay constants, quark masses and scale parameters in both models. We note that in the LFQM, the light quark masses in Eq. (5) are fixed by using the kaon decay constant $f_K = 159.8$ MeV and charge radius $\langle r_K^2 \rangle = 0.34$ fm^2, while in both models a different set of the heavy quark masses has little effect on the form factors.

Based on the parameters in Eqs. (5) and (6), we show the q^2 dependences of the form factors for $B_c^+ \to D^{(*)+}$ and $B_c^+ \to D_s^{(*)+}$ in Figs. 2 and 3, respectively. The numerical

TABLE I. Form factors for $B_c^+ \to D_{d,s}^{(*)+}$ transitions at $q^2=0$ in LFQM and CQM models, where $F_{\pm,T}$ are for $B_c^+ \to P^+(P=D,D_s)$ and $V,A_{0,\pm},g$ and $a_{0,+}$ for $B_c^+ \to V^+(V=D^*,D_s^*)$, respectively.

| | $B_c^+ \to D^{(*)+}$ | | | | $B_c^+ \to D_s^{(*)+}$ | | | |
| | LFQM | CQM | | | LFQM | CQM | | |
	$F_i(0)$	$F_i(0)$	σ_1	σ_2	$F_i(0)$	$F_i(0)$	σ_1	σ_2
F_+	0.126	0.123	-3.35	3.03	0.165	0.167	-3.40	3.21
F_-	-0.141	-0.130	-3.63	3.55	-0.186	-0.166	-3.51	3.38
F_T	-0.199	-0.186	-3.52	3.38	-0.258	-0.247	-3.41	3.30
V	-0.208	-0.198	-3.63	3.65	-0.336	-0.262	-3.49	3.51
A_0	-0.198	-0.198	-2.81	2.53	-0.330	-0.280	-2.66	2.24
A_+	0.079	0.108	-3.12	2.94	0.118	0.144	-2.99	2.95
A_-	-0.098	-0.185	-3.45	3.54	-0.130	-0.246	-3.34	3.46
g	0.130	0.124	-3.63	3.65	0.214	0.167	-3.45	3.29
a_0	0.130	0.124	-2.82	2.53	0.214	0.167	-2.63	2.23
a_+	-0.130	-0.124	-3.31	3.14	-0.214	-0.167	-3.16	3.13
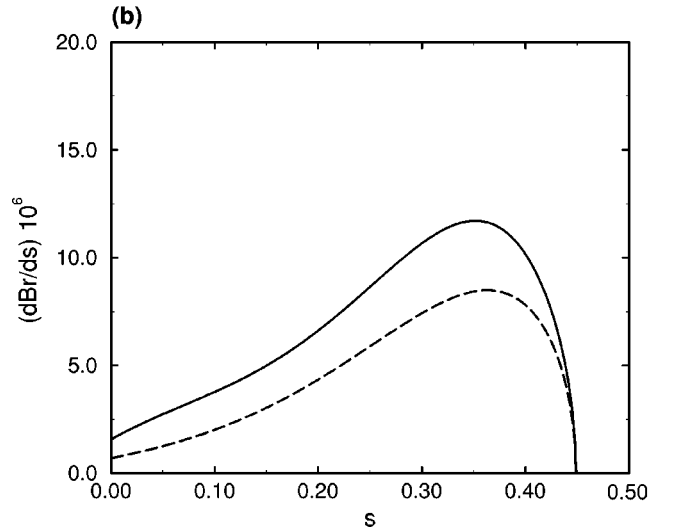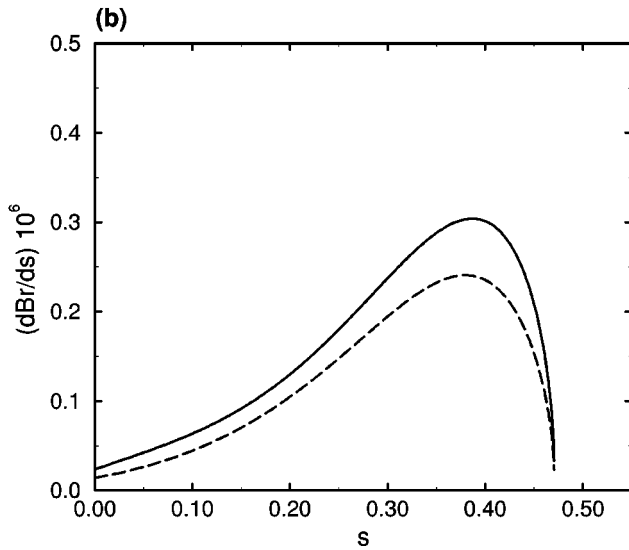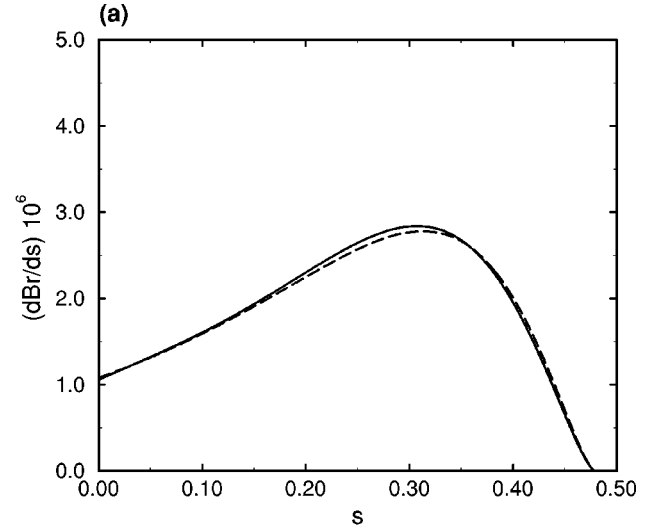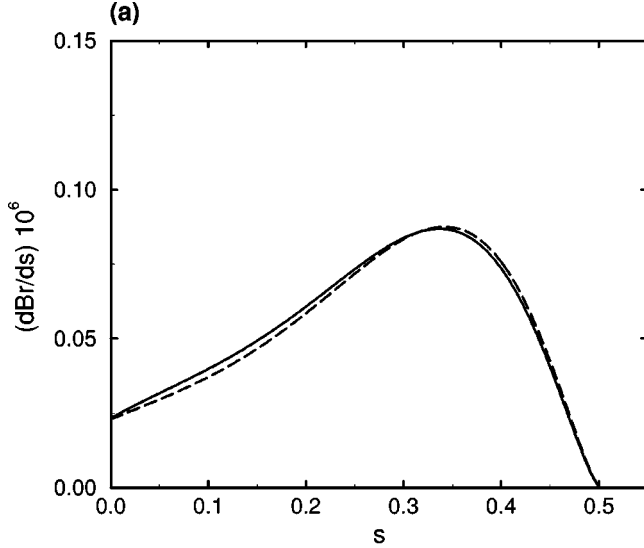
FIG. 4. Differential decay branching ratios as a function of $s = q^2/m_{B_c}^2$ for (a) $B_c^+ \to D^+ \nu\bar{\nu}$ and (b) $B_c^+ \to D^* \nu\bar{\nu}$. Legend is the same as Fig. 2.

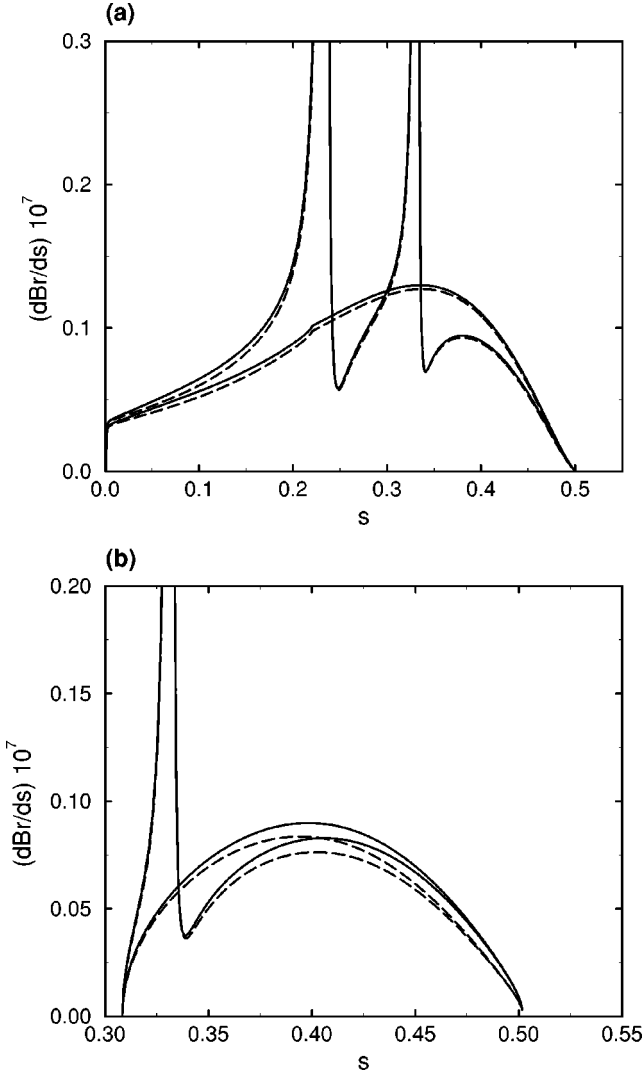FIG. 5. Same as Fig. 4 but for (a) $B_c^+ \to D_s^+ \nu\bar{\nu}$ and (b) $B_c^+ \to D_s^{+*} \nu\bar{\nu}$.

FIG. 6. Same as Fig. 4 but for (a) $B_c^+ \to D^+ \mu^+ \mu^-$ and (b) $B_c^+ \to D^+ \tau^+ \tau^-$. The curves with and without resonant shapes represent including and nonincluding LD contributions, respectively.

results for the form factors at $q^2=0$ are listed in Table I. From the table, we see that the values of the form factors at $q^2=0$ in the LFQM and CQM agree well with each other except $A_\pm(0)$. However, as shown in Figs. 2 and 3, the results at large q^2 in the two models are quite different.

III. DECAY RATES AND BRANCHING RATIOS

In the SM, the contributions to the rare decays of $B_c^+ \to D_{d,s}^{(*)+} l \bar{l}$ arise from the W-box and $Z(\gamma)$-penguin diagrams as seen in Fig. 1. The effective Hamiltonians of $b \to q \nu \bar{\nu}$ $(q=s,d)$ are given by [26]

$$\mathcal{H} = \frac{G_F}{\sqrt{2}} \frac{\alpha_{em}}{2\pi \sin^2\theta_W} \lambda_t D(x_t) \bar{b} \gamma_\mu (1-\gamma_5) q \bar{\nu} \gamma_\mu$$
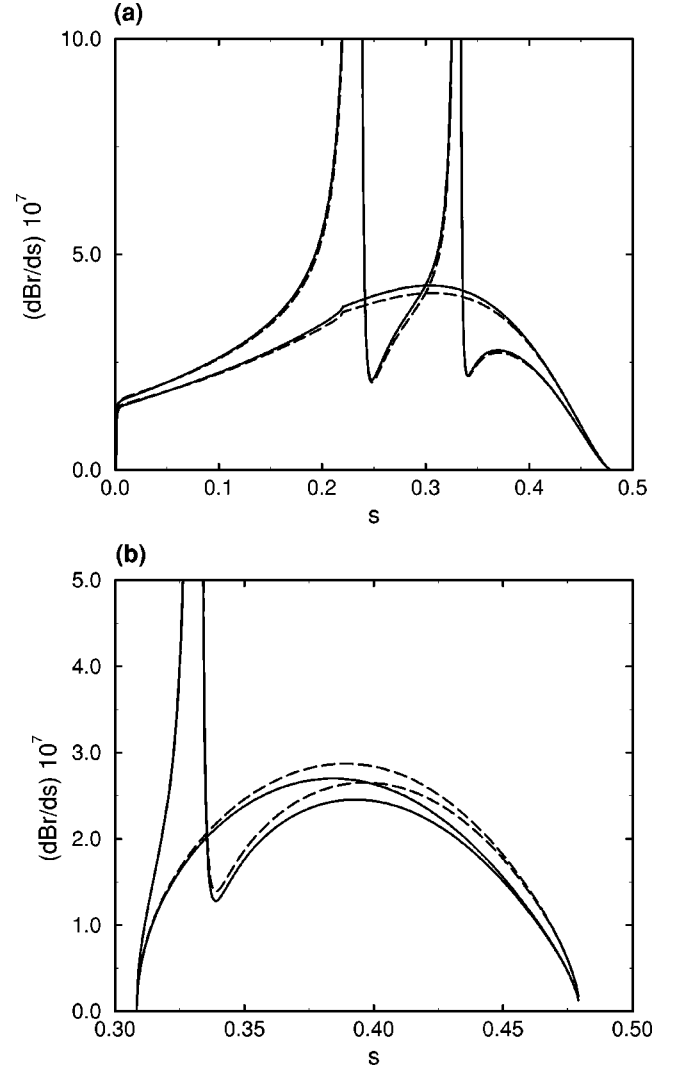$$\times (1-\gamma_5)\nu \tag{7}$$

FIG. 7. Same as Fig. 6 but for (a) $B_c^+ \to D_s^+ \mu^+ \mu^-$ and (b) $B_c^+ \to D_s^+ \tau^+ \tau^-$.

where G_F is the Fermi constant, $x_t \equiv m_t^2/m_W^2$, $\lambda_t = V_{tb}V_{tq}^*$ is the product of the CKM elements, and the m_t dependent function of $D(x_t)$ can be found in Refs. [27,28].

The effective Hamiltonians of $b \to q l^+ l^-$ $(q=s,d)$ are given by [26]

$$\mathcal{H} = \frac{G_F \alpha_{em} \lambda_t}{\sqrt{2}\pi} \left[C_8(\mu) \bar{s}_L \gamma_\mu b_L \bar{l} \gamma^\mu l + C_9 \bar{s}_L \gamma_\mu b_L \bar{l} \gamma^\mu \gamma_5 l \right.$$
$$\left. - \frac{2 m_b C_7(\mu)}{q^2} \bar{s}_L i \sigma_{\mu\nu} q^\nu b_R \bar{l} \gamma^\mu l \right] \tag{8}$$

where $C_8(\mu)$, C_9 and $C_7(\mu)$ are Wilson coefficients (WCs) and their expressions can be found in Ref. [28] for the SM. We note that C_9 is free of the μ scale. Besides the short-distance (SD) contributions, the main effect on the decays is from $c\bar{c}$ resonant states such as Ψ and Ψ', i.e., the long-

FIG. 8. Same as Fig. 6 but for (a) $B_c^+ \rightarrow D^{*+} \mu^+ \mu^-$ and (b) $B_c^+ \rightarrow D^{*+} \tau^+ \tau^-$.
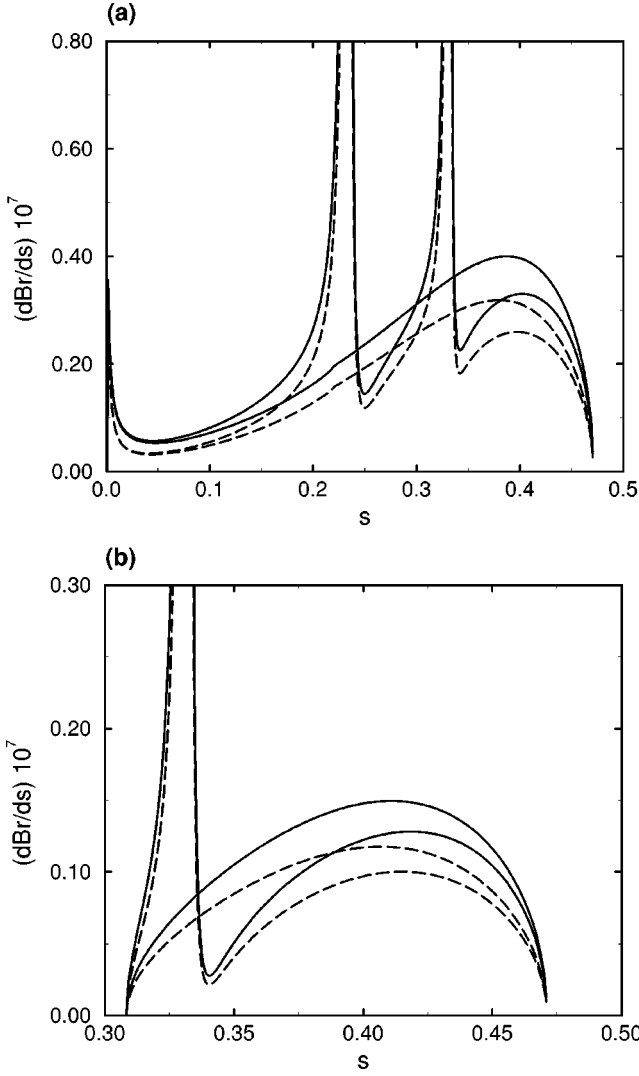

FIG. 9. Same as Fig. 6 but for (a) $B_c^+ \rightarrow D_s^{*+} \mu^+ \mu^-$ and (b) $B_c^+ \rightarrow D_s^{*+} \tau^+ \tau^-$.

distance (LD) contributions. To include the LD effect, in Eq. (8) we replace $C_8(\mu)$ by $C_8^{eff}(\mu)$ [28,29], given by

$$C_8^{eff}(\mu) = C_8(\mu) + (3C_1(\mu) + C_2(\mu))$$

$$\times \left(h(x,s) + \frac{3}{\alpha^2} \sum_{j=\Psi,\Psi'} k_j \frac{\pi \Gamma(j \rightarrow l^+ l^-) M_j}{q^2 - M_j^2 + i M_j \Gamma_j} \right),$$

$$(9)$$

where we have neglected the small WCs, and $h(x,s)$ describes the one-loop matrix elements of operators $O_1 = \bar{s}_\alpha \gamma^\mu P_L b_\beta \bar{c}_\beta \gamma_\mu P_L c_\alpha$ and $O_2 = \bar{s} \gamma^\mu P_L b \bar{c} \gamma_\mu P_L c$ [28], M_j (Γ_j) are the masses (widths) of intermediate states, and $k_j = -1/(3C_1(\mu) + C_2(\mu))$ [29].

From Eqs. (7) and (8), the differential decay rates for $B_c^+ \rightarrow H l\bar{l}(H = P, V)$ are found to be [30,31]
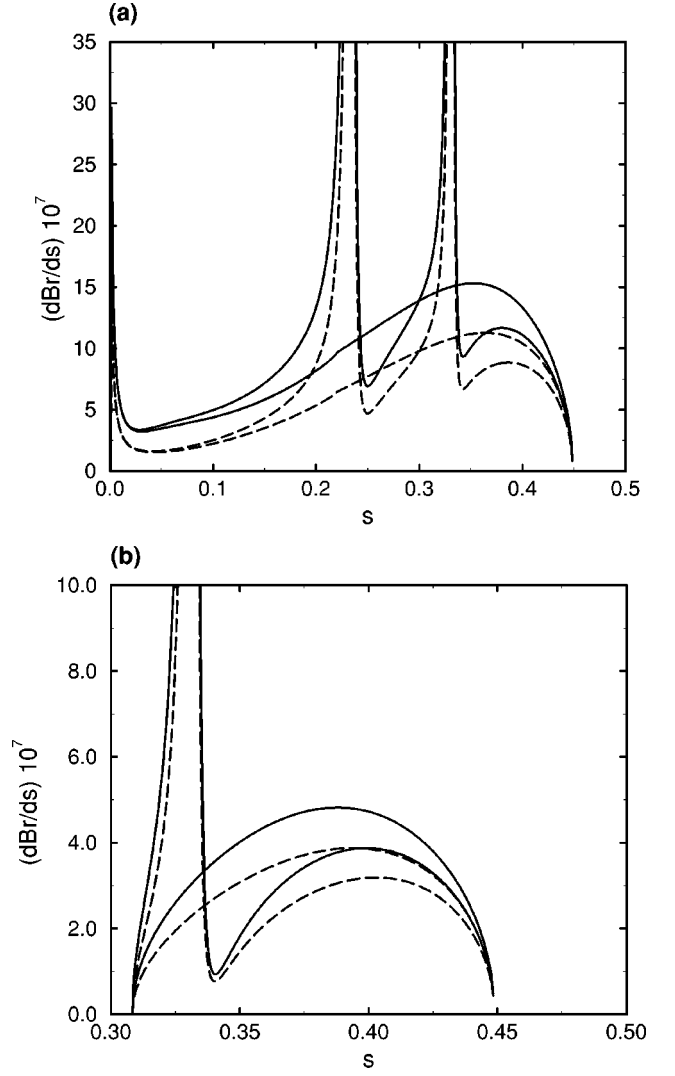
$$\frac{d\Gamma(B_c^+ \rightarrow P\nu\bar{\nu})}{ds} = \frac{G_F^2 m_{B_c}^5 |\lambda_t|^2 \alpha_{em}^2 |D(x_t)|^2}{2^8 \pi^5 \sin^4 \theta_W}$$

$$\times |F_+|^2 \phi_H^{3/2}, \qquad (10)$$

$$\frac{d\Gamma(B_c^+ \rightarrow V\nu\bar{\nu})}{ds} = \frac{3 G_F^2 m_{B_c}^5 |\lambda_t|^2 \alpha_{em}^2 |D(x_t)|^2}{2^8 \pi^5 \sin^4 \theta_W}$$

$$\times \phi_H^{1/2} \left[s \alpha_1 + \frac{\phi_H}{3} \beta_1 \right], \qquad (11)$$

$$\frac{d\Gamma(B_c^+ \rightarrow Pl^+ l^-)}{ds} = \frac{G_F^2 |\lambda_t|^2 m_{B_c}^5 \alpha_{em}^2}{3 \times 2^9 \pi^5} v \phi_H^{1/2}$$

$$\times \left[\left(1 + \frac{2t}{s} \right) \phi_H \alpha_2 + 12t \beta_2 \right], \quad (12)$$

TABLE II. Decay branching ratios of $B_c^+ \to D_{d,s}^{(*)+} \nu\bar{\nu}$.

	LFQM	CQM
$10^8 \mathrm{Br}(B_c^+ \to D^+ \nu\bar{\nu})$	2.77	2.74
$10^8 \mathrm{Br}(B_c^+ \to D^{*+} \nu\bar{\nu})$	7.64	5.99
$10^6 \mathrm{Br}(B_c^+ \to D_s^+ \nu\bar{\nu})$	0.92	0.92
$10^6 \mathrm{Br}(B_c^+ \to D_s^{*+} \nu\bar{\nu})$	3.12	2.12

and

$$\frac{d\Gamma(B_c^+ \to Vl^+l^-)}{ds} = \frac{G_F^2 m_{B_c}^5 |\lambda_t|^2 \alpha_{em}^2}{2^9 \pi^5} v \phi_H^{1/2}$$

$$\times \left[\left(1 + \frac{2t}{s} \right) \left(s\alpha_3 + \frac{\phi_H}{3} \beta_3 \right) + 4t\delta \right],$$

(13)

respectively, where $s = q^2/m_{B_c}^2$, $t = m_l^2/m_{B_c}^2$, $r_H = m_H^2/m_{B_c}^2$, $v = \sqrt{1 - 4t/s}$, and the expressions of ϕ_H, α_i, β_i [30] and δ [31] are given in the Appendix.

By using the form factors of the LFQM and CQM in Figs. 2 and 3, Eqs. (10)–(13), and $|\lambda_t| = |V_{tb} V_{tq}| = 0.041(0.008)$ for $q = s(d)$ [32], we now estimate the numerical values of the decay rates for $B_c^+ \to D_{d,s}^{(*)+} \nu\bar{\nu}$ and $B_c^+ \to D_{d,s}^{(*)+} l^+ l^-$. Our results for the differential decay branching ratios as a function of s are shown in Figs. 4–9, respectively. Here, for the charged lepton modes, we have presented our studies both with and without long-distance contributions. We note that the results for the electron modes are the same as the corresponding muon ones. We also note that at the large q^2 region, all the rates in the figures decrease because ϕ_H go to zero as $q^2 \to (m_b - m_{d,s})^2$. We emphasize that all our numerical predictions should be viewed as central values and their errors depend on the uncertainties from the corresponding meson decay constants and constituent quark masses as well as the Cabibbo-Kobayashi-Maskawa (CKM) parameters.

The decay branching ratios of $B_c^+ \to D_{d,s}^{(*)+} \nu\bar{\nu}$ and $B_c^+ \to D_{d,s}^{(*)+} l^+ l^- (l = \mu, \tau)$ are summarized in Tables II and III, respectively, where LD effects for the charged lepton modes are not included. With the LD effects, we introduce some cuts close to $q^2 = 0$ and around the resonances of J/ψ and ψ' and study the three regions as follows:

$$\mathrm{I}: \sqrt{q_{min}^2} < \sqrt{q^2} < M_{J/\psi} - 0.20;$$

$$\mathrm{II}: M_{J/\psi} + 0.04 < \sqrt{q^2} < M_{\psi'} - 0.10;$$

$$\mathrm{III}: M_{\psi'} + 0.02 < \sqrt{q^2} < m_{B_c} - m_{P,V},$$

(14)

TABLE III. Decay branching ratios of $B_c^+ \to D_{d,s}^{(*)+} l^+ l^-$ without including LD effects.

Decay mode	Without LD	
	LFQM	CQM
$10^8 \mathrm{Br}(B_c^+ \to D^+ \mu^+ \mu^-)$	0.41	0.40
$10^8 \mathrm{Br}(B_c^+ \to D^{*+} \mu^+ \mu^-)$	1.01	0.79
$10^8 \mathrm{Br}(B_c^+ \to D^+ \tau^+ \tau^-)$	0.13	0.12
$10^8 \mathrm{Br}(B_c^+ \to D^{*+} \tau^+ \tau^-)$	0.18	0.14
$10^7 \mathrm{Br}(B_c^+ \to D_s^+ \mu^+ \mu^-)$	1.36	1.33
$10^7 \mathrm{Br}(B_c^+ \to D_s^{*+} \mu^+ \mu^-)$	4.09	2.81
$10^7 \mathrm{Br}(B_c^+ \to D_s^+ \tau^+ \tau^-)$	0.34	0.37
$10^7 \mathrm{Br}(B_c^+ \to D_s^{*+} \tau^+ \tau^-)$	0.51	0.41

where $\sqrt{q_{min}^2} = 2m_l$ and 0.5 GeV for $B_c^+ \to D_{d,s}^+ l^+ l^-$ and $B_c^+ \to D_{d,s}^{*+} l^+ l^-$, respectively. In Table IV, we present the decay branching ratios in terms of the regions shown in Eq. (14).

As seen from Figs. 4–9 and Tables II–IV, the branching ratios of $B_c^+ \to D_{d,s}^+ l\bar{l}$ in the LFQM and CQM agree very well, while the results of $B_c^+ \to D_{d,s}^{*+} l\bar{l}$ in the LFQM are larger than those in the CQM but the differences are at the 20% level.

Finally, we remark that in our calculations on $B_c^+ \to D_q^{*+} l^+ l^- (q = d,s)$, we have not included the contributions from the weak annihilation accompanied by a photon emission which are dominant in the decays of $B_c^+ \to D_q^{*+} \gamma$ [9]. However, they are only important at low s and the cut at $\sqrt{q_{min}^2}$ in Eq. (14) should reduce the contributions from the virtual photon diagrams.

IV. CONCLUSIONS

We have studied the rare B_c decays of $B_c^+ \to D_{d,s}^{(*)+} \nu\bar{\nu}$ and $B_c^+ \to D_{d,s}^{(*)+} l^+ l^-$ $(l = e, \mu, \tau)$. In our analysis, we have used the form factors of $B_c^+ \to D_{d,s}^{(*)+}$ transitions calculated in the LFQM and CQM. We have found that $Br(B_c^+ \to D^+ l\bar{l})(l = \nu, e, \mu, \tau) = (2.77, 0.41, 0.41, 0.13)$ and $(2.74, 0.40, 0.40, 0.12) \times 10^{-8}$, $Br(B_c^+ \to D_s^+ l\bar{l}) = (9.2, 1.36, 1.36, 0.34)$ and $(9.2, 1.33, 1.33, 0.37) \times 10^{-7}$, $Br(B_c^+ \to D^{*+} l\bar{l}) = (7.64, 1.01, 1.01, 0.18)$ and $(5.99, 0.79, 0.79, 0.14) \times 10^{-8}$, and $Br(B_c^+ \to D_s^{*+} l\bar{l}) = (31.2, 4.09, 4.09, 0.51)$ and $(21.2, 2.81, 2.81, 0.41) \times 10^{-7}$, in the two models, respectively. Clearly, some of the above rare B_c decays can be measured at the BTeV and LHC-B experiments.

TABLE IV. Decay branching ratios of $B_c^+ \to D_{d,s}^{(*)+} l^+ l^-$ with LD effects and the cuts.

| | With LD | | | | | | | |
| Regions | I | | II | | III | | I+II+III | |
Decay mode	LFQM	CQM	LFQM	CQM	LFQM	CQM	LFQM	CQM
$10^9 \mathrm{Br}(B_c^+ \to D^+ \mu^+ \mu^-)$	1.48	1.40	0.75	0.73	1.09	1.07	3.31	3.20
$10^9 \mathrm{Br}(B_c^+ \to D^{*+} \mu^+ \mu^-)$	2.17	1.55	1.81	1.49	3.78	2.95	7.75	5.98
$10^9 \mathrm{Br}(B_c^+ \to D^+ \tau^+ \tau^-)$			0.02	0.01	1.03	0.94	1.05	0.95
$10^9 \mathrm{Br}(B_c^+ \to D^{*+} \tau^+ \tau^-)$			0.02	0.02	1.30	1.02	1.33	1.03
$10^8 \mathrm{Br}(B_c^+ \to D_s^+ \mu^+ \mu^-)$	5.89	5.83	2.57	2.47	2.69	2.66	11.15	10.96
$10^8 \mathrm{Br}(B_c^+ \to D_s^{*+} \mu^+ \mu^-)$	11.90	6.80	8.30	5.78	11.18	8.58	31.38	21.16
$10^8 \mathrm{Br}(B_c^+ \to D_s^+ \tau^+ \tau^-)$			0.05	0.05	2.67	2.95	2.72	3.00
$10^8 \mathrm{Br}(B_c^+ \to D_s^{*+} \tau^+ \tau^-)$			0.10	0.08	3.31	2.73	3.41	2.80

APPENDIX

The parameters of ϕ_H, α_i, $\beta_i (i=1,2,3)$ and δ in Eqs. (10)–(13) are defined by

$$\phi_H = (1-r_H)^2 - 2s(1+r_H) + s^2, \tag{A1}$$

$$\alpha_1 = (1-\sqrt{r_H})^2 |A_0|^2 + \frac{\phi_H}{(1+\sqrt{r_H})^2}|V|^2, $$

$$\beta_1 = \frac{(1-\sqrt{r_H})^2}{4r_H}|A_0|^2 - \frac{s}{(1+\sqrt{r_H})^2}|V|^2 + \frac{\phi_H |A_+|^2}{4r_H(1+\sqrt{r_H})^2} + \frac{1}{2}\left(\frac{1-s}{r_H}-1\right)\frac{1-\sqrt{r_H}}{1+\sqrt{r_H}}\mathrm{Re}(A_0 A_+^*), \tag{A2}$$

$$\alpha_2 = \left|C_8^{eff} F_+ - \frac{2\hat{m}_b C_7 F_T}{1+\sqrt{r_H}}\right|^2 + |C_9 F_+|^2, $$

$$\beta_2 = |C_9|^2 \left[\left(1+r_H - \frac{s}{2}\right)|F_+|^2 + (1-r_H)\mathrm{Re}(F_+ F_-^*) + \frac{1}{2}s|F_-|^2\right], \tag{A3}$$

$$\alpha_3 = (1-\sqrt{r_H})^2 \left[\left|C_8^{eff} A_0 - \frac{2\hat{m}_b C_7 (1+\sqrt{r_H})a_0}{s}\right|^2 + |C_9 A_0|^2\right] + \frac{\phi_H}{(1+\sqrt{r_H})^2}\left[\left|C_8^{eff} V - \frac{2\hat{m}_b C_7 (1+\sqrt{r_H})g}{s}\right|^2 + |C_9 V|^2\right], $$

$$\beta_3 = \frac{(1-\sqrt{r_H})^2}{4r_H}\left[\left|C_8^{eff} A_0 - \frac{2\hat{m}_b C_7 (1+\sqrt{r_H})a_0}{s}\right|^2 + |C_9 A_0|^2\right] - \frac{s}{(1+\sqrt{r_H})^2}\left[\left|C_8^{eff} V - \frac{2\hat{m}_b C_7 (1+\sqrt{r_H})g}{s}\right|^2 + |C_9 V|^2\right]$$

$$+ \frac{\phi_H}{4r_H(1+\sqrt{r_H})^2}\left[\left|C_8^{eff} A_+ - \frac{2\hat{m}_b C_7 (1+\sqrt{r_H})a_+}{s}\right|^2 + |C_9 A_+|^2\right] + \frac{1}{2}\left(\frac{1-s}{r_H}-1\right)\frac{1-\sqrt{r_H}}{1+\sqrt{r_H}}$$

$$\times \mathrm{Re}\left\{\left[C_8^{eff} A_0 - \frac{2\hat{m}_b C_7 (1+\sqrt{r_H})a_0}{s}\right]\left[C_8^{eff} A_+ - \frac{2\hat{m}_b C_7 (1+\sqrt{r_H})a_+}{s}\right] + |C_9|^2 \mathrm{Re}(A_0 A_+^*)\right\}, \tag{A4}$$

and

$$\delta = \frac{|C_9|^2}{2(1+\sqrt{r_H})^2}\left\{-2\phi_H |V|^2 - 3(1-r_H)^2 |A_0|^2 + \frac{\phi_H}{4r_H}[2(1+r_H)-s]|A_+|^2 + \frac{\phi_H s}{4r_H}|A_-|^2 + \frac{\phi_H(1-r_H)}{2r_H}\right.$$

$$\left.\times \mathrm{Re}(A_0 A_+^* + A_0 A_-^* + A_+ A_-^*)\right\}, \tag{A5}$$

respectively, where $\hat{m}_b = m_b / m_{B_c}$.

[1] CDF Collaboration, F. Abe *et al.*, Phys. Rev. D **58**, 112004 (1998); Phys. Rev. Lett. **81**, 2432 (1998).

[2] Particle Data Group, D.E. Groom *et al.*, Eur. Phys. J. C **15**, 1 (2000).

[3] N. Isgur and M.B. Wise, Phys. Lett. B **232**, 113 (1989); **237**, 527 (1990).

[4] For a recent review, see A. Ali *et al.*, Phys. Rev. D **61**, 074024 (2000).

[5] CLEO Collaboration, M.S. Alam *et al.*, Phys. Rev. Lett. **74**, 2885 (1995).

[6] Belle Collaboration, K. Abe *et al.*, Phys. Rev. Lett. **88**, 021801 (2002).

[7] C.-H. Chang and Y.-Q. Chen, Phys. Rev. D **49**, 3399 (1994); A. Abd El-Hady, J.H. Muõz, and J.P. Vary, *ibid.* **62**, 014019 (2000); A.Yu. Anisimov, P.Yu. Kulikov, I.M. Narodetskii, and K.A. Ter-Martirosyan, Phys. At. Nucl. **62**, 1739 (1999); V.V. Kiselev, A.K. Likhoded, and A.I. Onishchenko, Nucl. Phys. **B259**, 473 (2000); V.V. Kiselev, A.E. Kovalsky, and A.K. Likhoded, *ibid.* **B585**, 353 (2000); P. Colangelo and F. De Fazio, Phys. Rev. D **61**, 034012 (2000).

[8] M.A. Ivanov, J.G. Körner, and P. Santorelli, Phys. Rev. D **63**, 074010 (2001); and references therein.

[9] D.S. Du, Xiu-lin Li, and Ya-dong Yang, Phys. Lett. B **380**, 193 (1996); G.R. Lu *et al.*, Phys. Rev. D **54**, 5647 (1996); N. Barik, Sk. Naimuddin, S. Kar, and P.C. Dash, *ibid.* **63**, 014024 (2001).

[10] C.C. Lih, C.Q. Geng, and W.M. Zhang, Phys. Rev. D **59**, 114002 (1999); C.Q. Geng, C.C. Lih, and T.H. Wu, *ibid.* **60**, 054002 (1999).

[11] D.S. Du and Z. Wang, Phys. Rev. D **39**, 1342 (1989); C.H. Chang and Y.Q. Chen, *ibid.* **48**, 4086 (1993); K. Cheung, Phys. Rev. Lett. **71**, 3413 (1993); E. Braaten, K. Cheung, and T. Yuan, Phys. Rev. D **48**, R5049 (1993).

[12] For a review, see, e.g., S. Stone, hep-ph/9709500.

[13] J.M. Flynn and C.T. Sachrajda, hep-lat/9710057.

[14] E. Bagan *et al.*, Z. Phys. C **64**, 57 (1997).

[15] V.V. Kiselev, A.E. Kovalsky, and A.K. Likhoded, Nucl. Phys. **B585**, 353 (2000).

[16] H.Y. Cheng, C.Y. Cheung, and C.W. Hwang, Phys. Rev. D **55**, 1559 (1997).

[17] C.Q. Geng, C.W. Hwang, C.C. Lih, and W.M. Zhang, Phys. Rev. D **64**, 114024 (2001).

[18] D. Melikhov, N. Nikitin, and S. Simula, Phys. Rev. D **57**, 6814 (1998).

[19] D. Melikhov and B. Stech, Phys. Rev. D **62**, 014006 (2000).

[20] M.V. Terent'ev, Sov. J. Nucl. Phys. **24**, 106 (1976); V.B. Berestetsky and M.V. Terent'ev, *ibid.* **24**, 547 (1976); **25**, 347 (1977).

[21] P.L. Chung, F. Coester, and W.N. Polyzou, Phys. Lett. B **205**, 545 (1988).

[22] W.M. Zhang, Chin. J. Phys. (Taipei) **31**, 717 (1994); Report No. IP-ASTP-19-95, hep-ph/9510428.

[23] C.Y. Cheung, C.W. Hwang, and W.M. Zhang, Z. Phys. C **75**, 657 (1997); C.Q. Geng, C.C. Lih, and Wei-Min Zhang, Phys. Rev. D **57**, 5697 (1998); N.B. Demchuk, I.L. Grach, I.M. Narodetskii, and S. Simula, Yad. Fiz. **59**, 2235 (1996) [Phys. At. Nucl. **59**, 2152 (1996)]; I.L. Grach, I.M. Narodetskii, and S. Simula, Phys. Lett. B **385**, 317 (1996).

[24] A. Dubin and A. Kaidalov, Yad. Fiz. **56**, 164 (1993) [Phys. At. Nucl. **56**, 237 (1993)].

[25] D. Melikhov, Phys. Rev. D **53**, 2460 (1996).

[26] T. Inami and C.S. Lim, Prog. Theor. Phys. **65**, 297 (1981).

[27] G. Belanger and C.Q. Geng, Phys. Rev. D **43**, 140 (1991).

[28] G. Buchalla and A.J. Buras, Nucl. Phys. **B400**, 225 (1993).

[29] C.H. Chen and C.Q. Geng, Phys. Rev. D **63**, 114025 (2001); **64**, 074001 (2001).

[30] C. Breub, A. Ioannissian, and D. Wyler, Phys. Lett. B **346**, 149 (1995).

[31] C.Q. Geng and C.P. Kao, Phys. Rev. D **54**, 5636 (1996).

[32] See, e.g., A.J. Buras, hep-ph/0109197.